Transactions of the **14th International Conference on Structural Mechanics in Reactor Technology** (SMiRT 14), Lyon, France, August 17-22, 1997 **C03/4**

# Development of a methodology for in-reactor fuel rod supporting condition prediction

**Kim H.K., Kim K.T.**
*Korea Atomic Energy Research Institute, Korea*

## ABSTRACT

The in-reactor fuel rod support conditions against the fretting wear-induced damage can be evaluated by rod-to-grid gap. In order to evaluate the impact of fuel design parameters on the fretting wear-induced damage, a simulation methodology for the in-reactor fuel rod supporting conditions as a function of burnup has been developed and implemented in the GRIDFORCE program. This methodology was applied to the fretting wear-induced failure experienced in a commercial plant.

## NOMENCLATURE

$F_{RES}(t)$ = residual spring force at a time $t$
$C_{OT}$ = spring constant at operating temperature
$\delta_{RES}(t)$ = residual elastic spring deflection at a time $t$
$\delta_0$ = initial spring deflection at room temp.
$\delta_P(t)$ = elastic cladding deflection caused by the coolant overpressure at $t$
$\delta_T(t)$ = thermal expansion difference between the spacer grid strip and the cladding at $t$
$\delta_{CR}(t)$ = accumulated cladding creepdown from $0$ to $t$
$\delta_{IR}(t)$ = accumulated spacer grid irradiation growth from $0$ to $t$
$\delta_{REX}(t)$ = accumulated loss of spring deflection due to spring force relaxation from $0$ to $t$
$F_G(t)$ = spring force calculated by the geometrical configuration of cladding and spacer grid at $t = t$ without considering spring force relaxation
$R(t)$ = fraction of residual spring force to be relaxed from $0$ to $t$, which is obtained under a constant total(elastic + plastic) spring deflection condition
$F^W_{EFF}(t)$ = time-weighted spring force from $0$ to $t$
$\delta_G(t)$ = elastic spring deflection calculated by the geometrical configuration of cladding and spacer grid at $t = t$ without considering spring force relaxation
$(= \delta_0 - \delta_P(t) - \delta_T(t) - \delta_{CR}(t) - \delta_{IR}(t))$
superscript $^*$ indicates increment
superscript $^W$ indicates time weighted value from time $0$ to $t$
$\Delta t_j$ = time interval at the (j)th time step $(= t_j - t_{j-1})$

## 1. INTRODUCTION

One of the aims of fuel designs is the assurance of the fuel rod and fuel assembly integrity under the normal operating conditions. Due to fuel design and/or its specifications deficiency, manufacturing fault, fuel handling or operational mistake, however, fuel failures have occurred. In the 1970s, the main failure mechanisms are identified as hydriding, PCI and clad collapsing, which were eliminated by various corrective actions such as fuel design change and/or operational guideline improvement [1]. Nevertheless, fretting wear induced fuel failure still remains as one of the serious fuel failure mechanisms. Regarding the fretting wear problems, key factors can be divided into two groups such as fuel design parameters and reactor hydraulic design parameters. The fuel design parameters includes initial spring deflection, irradiation-induced spring force relaxation, cladding creepdown and thermal expansion difference between spacer grid and rod. The reactor hydraulic design parameters are assemblywise flow distribution, axial flow rate fluctuation in the fuel assembly and cross flow rate at the interfaces of fuel assembly/fuel assembly and fuel assembly/baffle. It is well known that the probability of the fretting wear damage may be reduced by smaller cladding creepdown and spring force relaxation, larger initial spring deflection and lower flow-induced vibration.

In this work, a simulation methodology of the rod-to-grid supporting conditions will be developed and implemented in the GRIDFORCE program. With the help of this program, the impact of the fuel design parameters on the rod-to-grid supporting conditions will be evaluated, based on the parametric study, and then possibility of the fretting wear damage will be estimated. However, the impact of the reactor hydraulic design parameters on the fretting wear damage under the given rod-to-grid supporting conditions will not be evaluated since up to now there have existed no in-reactor vibration-related data of the fuel rod and the fuel assembly needed for benchmarking it.

## 2. DESCRIPTION OF METHODOLOGY

It is well known that the fuel rod supporting conditions in a pressurized water reactor depend on the various parameters such as the cladding creep rate, the spacer grid design, and the coolant flow condition. In this work, however, only the effects of the cladding creep rate and the spacer grid design on the fretting wear-induced failure are considered. The cladding creep rate can be predicted by a fuel performance code with the consideration of the fuel rod power histories and the thermal-hydraulic conditions. The initial spring deflection and force are determined from the spring force-deflection curves which is governed by the spring design such as spring height, spring width and spring shape. The spring force relaxation depends on the residual stress in spring and the amount of fast fluence. The higher residual stress and the larger fast fluence will generate the larger spring force relaxation. It is noteworthy that the cladding creepdown rate has a direct impact on the spring relaxation rate since the former controls the rod-to-grid gap size, i.e., the residual stress in spring. The simulation methodology developed in this work, which takes into account the cladding creep rate, the spring stiffness, the initial spring deflection, the initial spring force, and the spring force relaxation rate, can be described as follows :

The residual spring force at a time $t$ at the operating temperature may be represented by the Hooke's law :

$$F_{RES}(t) = C_{OT}\,\delta_{RES}(t) \tag{1}$$

As shown in Fig.1, the initial spring elastic deflection at the room temperature, $\delta_0$, decreases due to the cladding elastic deflection caused by the coolant overpressure, $\delta_P$, and the thermal expansion difference between the spacer grid strip and the cladding, $\delta_T$. In addition, $\delta_0$ decreases with an increase of burnup due to the cladding creepdown, $\delta_{CR}$, the spacer grid strip irradiation growth, $\delta_{IR}$, and the spring force relaxation $\delta_{REX}$. With the combination of all the parameters described above, the residual elastic spring deflection at $t$, $\delta_{RES}(t)$, may be given in the followings :

$$\delta_{RES}(t) = \delta_0 - \delta_P(t) - \delta_T(t) - \delta_{CR}(t) - \delta_{IR}(t) - \delta_{REX}(t) \quad (2)$$

The value of $\delta_0$ can be determined by an unstrained spring height, fuel rod pitch and initial cladding diameter. With given operating conditions, $\delta_P(t)$, $\delta_T(t)$, $\delta_{CR}(t)$, and $\delta_{IR}(t)$ can be calculated by the reactor operating conditions. Since the total spring deflection is decreased due to cladding creepdown and/or spacer grid irradiation growth, however, the value of $\delta_{REX}(t)$ for the spacer grid spring contacting on the cladding can not be determined directly from a burnup-dependent relaxation curve which is obtained from the in-pile spring force relaxation tests under a constant total(elastic + plastic) spring deflection. In order to evaluate the impact of a burnup-dependent total spring deflection on the amount of the spring force relaxation, a time-weighted spring force may be introduced for the calculation of the residual spring force :

$$F_{RES}(t) = F_G(t) - [1 - R(t)]F^W_{EFF}(t) \quad (3)$$

Using the relationship of $F = C\,\delta$, equation (3) can be rewritten as

$$\delta_{RES} = \delta_G(t) - [1 - R(t)]\delta^W_{RES}(t) \quad (4)$$

Comparison of equation (2) and (4) shows

$$\delta_{REX}(t) = [1 - R(t)]\delta^W_{RES}(t) \quad (5)$$

With the introduction of time-weighted values of $\delta^W_P$, $\delta^W_T$, $\delta^W_{CR}$ and $\delta^W_{IR}$, $\delta^W_{RES}(t)$ can be given as :

$$\delta^W_{RES}(t) = \delta_0 - \delta^W_P(t) - \delta^W_T(t) - \delta^W_{CR}(t) - \delta^W_{IR}(t) \quad (6)$$

$\delta^W_P(t)$, $\delta^W_T(t)$, $\delta^W_{CR}(t)$ and $\delta^W_{IR}(t)$ may be derived as follows :

$$\delta^W_P(t) = \frac{1}{t}\int_0^t \delta^*_P(\tau)\left[\frac{t-\tau}{t}\right]d\tau \quad (7)$$

$$\delta^W_T(t) = \frac{1}{t}\int_0^t \delta^*_T(\tau)\left[\frac{t-\tau}{t}\right]d\tau \quad (8)$$

$$\delta^W_{CR}(t) = \frac{1}{t}\int_0^t \delta^*_{CR}(\tau)\left[\frac{t-\tau}{t}\right]d\tau \quad (9)$$

$$\delta^W_{IR}(t) = \frac{1}{t}\int_0^t \delta^*_{IR}(\tau)\left[\frac{t-\tau}{t}\right]d\tau \quad (10)$$

It is noted that in the above equations the weighting factor of $[t - \tau]$ is introduced to consider the impact of $\delta^*_P(\tau)$, $\delta^*_T(\tau)$, $\delta^*_{CR}(\tau)$ and $\delta^*_{IR}(\tau)$ on the amount of the spring force relaxation. This weighting factor represents an elapsed time from $t = \tau$ to $t = t$ after the appearance of $\delta^*_P(\tau)$, $\delta^*_T(\tau)$, $\delta^*_{CR}(\tau)$ and $\delta^*_{IR}(\tau)$ at $t = \tau$. In order to simplify the integration in the above equations, the time of $t$ is divided into N time intervals and then the integral given in the above equations can be transformed into a summation :

$$\delta_P^W(t) = \sum_{j=1}^{N} [\delta_P(j) - \delta_P(j-1)][t_N - (t_j - 1/2\,\Delta t_j)]/t_N \quad (11)$$

$$\delta_T^W(t) = \sum_{j=1}^{N} [\delta_T(j) - \delta_T(j-1)][t_N - (t_j - 1/2\,\Delta t_j)]/t_N \quad (12)$$

$$\delta_{CR}^W(t) = \sum_{j=1}^{N} [\delta_{CR}(j) - \delta_{CR}(j-1)][t_N - (t_j - 1/2\,\Delta t_j)]/t_N \quad (13)$$

$$\delta_{IR}^W(t) = \sum_{j=1}^{N} [\delta_{IR}(j) - \delta_{IR}(j-1)][t_N - (t_j - 1/2\,\Delta t_j)]/t_N \quad (14)$$

Then, substitution of equation (6) and equations (11) through (14) into equation (5) gives

$$\delta_{RES}(t) = \delta_G(t) - [1 - R(t)][\delta_0 - \delta_P^W(t) - \delta_T^W(t) - \delta_{CR}^W(t) - \delta_{IR}^W(t)] \quad (15)$$

The above equations (1) through (15) have been implemented into the GRIDFORCE computer program. With an aid of this program, the fuel rod supporting conditions as a function of burnup can be easily predicted when the fuel assembly design parameters are known.

## 3. APPLICATIONS AND PARAMETRIC STUDY

### 3.1 *Applications*

The GRIDFORCE program has been utilized to predict the fretting wear-induced failures experienced in a Korean nuclear power plant. According to the fretting wear-induced failures observed in the nuclear power plant, the fuel has experienced the fretting wear-induced fuel failure during the second residence time. The first symptom of the fuel damage due to the fretting wear occurred at 20-23 MWD/kgU, which corresponds to about 100 days after the startup of the second residence time. According to the visual examination of the fuel rod, it appears that the rod-to-grid gap initiated at the middle spacer grid positions and propagated in upper and lower spacer grid positions with an increase of burnup. Due to the different flow-induced vibration in the core and the fuel assembly, however, some fuel rods even in the failed fuel assemblies and some fuel assemblies located at the symmetric positions of the failed fuel assemblies have remained intact. Fig.2 summarizes the fretting wear depth profile versus spacer grid position. With an aid of the GRIDFORCE program, the residual elastic spring deflections for the fuel were predicted at various spacer grid positions, as shown in Fig. 3. From this figure, the GRIDFORCE program predicts that the rod-to-grid gap initiates at the middle spacer grid positions at the burnup of 20 MWD/kgU and then propagates in upper and lower directions with an increase of burnup. It is known that for Inconel spacer grid the rod-to-grid gap will not be allowed in order to eliminate the fretting wear damage. Since Inconel spacer grid has been employed for the fuel considered in this work, therefore, the GRIDFORCE program is considered to predict well the residual elastic spring deflection and the rod-to-grid gap at various spacer grid positions as a function of burnup.

### 3.2 *Parametric Study*

With an aid of the GRIDFORCE program containing the simulation model developed in this work, the parametric studies on the key parameters of the fuel rod supporting conditions such as the cladding creepdown, the initial spring deflection, the initial spring force, and the

spring force relaxation have been performed. The spring characteristic curves of the typical spring designs employed in this work are given in Fig. 4. From this figure, it can be seen that depending on spring type the spring deflection range varies from 0.3 to 1.0 mm and the initial spring force range varies from 10 to 27 N. The typical spring force relaxation rates are given in Fig.5. Depending on the spring design, the remaining fractional spring force at 8x1021 n/cm$^2$ varies from 0.3 to 0.1. The typical creepdown behaviors of the cladding tubes supplied to the Korean plants are given in Fig.6. These curves indicate that the lower tin content generates the faster creepdown. Based on the given data in Figs.4 through 6, the GRIDFORCE program can evaluate the effect of each parameters on the fuel rod supporting conditions. In this work, the fuel rod supporting conditions at the middle spacer grid position have been investigated since the fretting wear-induced fuel damage caused by insufficient initial spring deflection started at the middle spacer grid position, as shown in Fig. 2.

### 3.2.1 *Initial Spring Deflection*

Fig.4 shows the spring deflection-force curves employed in this work. In order to evaluate the effect of the initial spring deflection only on the fuel rod supporting conditions, the spring type 2 was selected. From Fig.4, it can be seen that the tolerance range of spring deflection is from 0.3 to 1.0 mm. As an input datum in the GRIDFORCE program, three initial spring deflections of 0.3, 0.6, 1.0 mm were selected from the tolerance range of the spring type 2. The results for the effect of the initial spring deflection is shown in Fig.7. From this figure, it can be seen that the larger spring deflection generates the larger residual spring deflection, as expected. The initial spring deflection of 0.3 mm generates gap from fuel rod burnup of 32 MWD/kgU, whereas the initial spring deflection of 1.0 mm does not generates gap and residual spring deflection is saturated to be 0.1 mm from 38 MWD/kgU. Therefore, it is recommended that the lower tolerance range of spring deflection for new spring designs be checked whether or not the gap between the fuel rod and the spacer grid will occur during the fuel lifetime, which can be easily checked by the GRIDFORCE program.

### 3.2.2 *Initial Spring Force*

In order to evaluate the effect of the initial spring deflection only on the fuel rod supporting conditions, the same relaxation curve and cladding creepdown were employed regardless of spring design. As an input datum in the GRIDFORCE program, three initial spring forces of 7, 10, 15 N with the same spring deflection of 0.3 mm were selected from Fig.4. The results for the effect of the initial spring force is shown in Fig.8. From this figure, it can be seen that there is nearly no effect of the initial spring force on the residual spring deflection behavior. According to the results predicted by the GRIDFORCE program, it can be said that, in order to improve the spacer grid design against the fretting wear-induced failure, one should increase the initial spring deflection rather than the initial spring force.

### 3.2.3 *Spring Force Relaxation*

Three kinds of spring force relaxation rate used in this work are given in Fig.5. In order to evaluate the effect of the spring force relaxation only on the fuel rod supporting conditions,

the same initial spring deflection and cladding creepdown were employed regardless of the spring force relaxation. As an input datum in the GRIDFORCE program, three spring force relaxation rates were selected from Fig.5. The results for the effect of the spring force relaxation is shown in Fig.9. From this figure, it can be seen that the smaller spring force relaxation generates the larger residual spring deflection, as expected. The spring relaxation types B and C generate gap from the fuel rod burnup of 33 and 26 MWD/kgU, respectively, whereas the spring relaxation type A does not generates gap and residual spring deflection is saturated to be 0.02 mm from 38 MWD/kgU. According to the results predicted by the GRIDFORCE program, it can be said that, in order to improve the spacer grid design against the fretting wear-induced failure, one should reduce the spring force relaxation as small as possible. Considering that the higher local stress in the spring generates the faster spring force relaxation, it is recommended that local stress in the spring be reduced by optimizing spring shape.

### 3.2.4 *Cladding Creepdown*

Three cladding creepdown curves used in this work are given in Fig.6. In order to evaluate the effect of the cladding creepdown only on the fuel rod supporting conditions, the same initial spring deflection and spring force relaxation were employed. As an input datum in the GRIDFORCE program, three cladding creepdowns were selected from Fig.6. The results for the effect of the cladding creepdown is shown in Fig.10. From this figure, it can be seen that the smaller cladding creepdown generates the larger residual spring deflection, as expected. The extra low tin cladding generates gap from the fuel rod burnup of 30 MWD/kgU, whereas the high tin cladding generates gap from the fuel rod burnup of 35 MWD/kgU. Comparison of the effect of each parameter on the residual spring deflection indicates that the most important parameter is the initial spring deflection and the second one is the spring force relaxation. It also indicates that the initial spring force does not affect the residual spring deflection behavior if the same initial spring deflection is assumed. In order to optimize the spacer grid design against the fretting wear-induced failure, therefore, one should have a spacer grid design of relatively low spring force but large spring deflection since it is generally known that the larger initial spring force shows the faster spring force relaxation due to higher local stress in the spring. In addition, one should use the cladding material with small creepdown rate if the other performance parameters such as oxidation and irradiation growth are not concerned.

## 4. CONCLUSIONS

A simulation methodology for the evaluation of the impact of the fuel design on the fuel rod support conditions has been developed and implemented in the GRIDFORCE program. The GRIDFORCE program has been considered to predict well the fuel rod supporting conditions at various spacer grid positions as a function of burnup. Based on the parametric studies, it is found that the most dominant parameter for the residual spring deflection is the initial spring deflection and the second one is the spring force relaxation. It is also found that the initial spring force does not affect the residual spring deflection behavior. In order to optimize the existing spacer grid designs and/or develop new spacer grid designs, the GRIDFORCE program can be employed as an effective tool since it will check whether or not

a proposed spacer grid design can prevent the fretting wear-induced damage.

## REFERENCES


1. P. Knudsen 1979. Evaluation of LWR fuel performance under transient and off-normal conditions. A Review of Recent Reports, RISO-M-2211.
2. Washington 1993. Fuel failure at two plants force Westinghouse to redesign VANTAGE5H. *Nuclear fuel,* 18.
3. Borsdorf 1993. Verification of fuel rod support in fuel assemblies with Inconel spacer grids type AH42. KWU BT52/93/E346.
4. Manual for a Computer Code CARO-D, Fuel Performance Analysis Code.


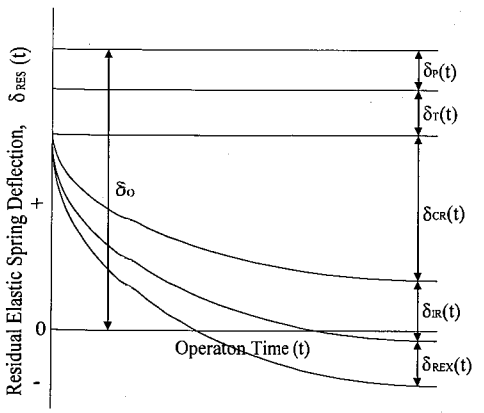


Fig.1 Schematic diagram of residual elastic spring deflection versus time.

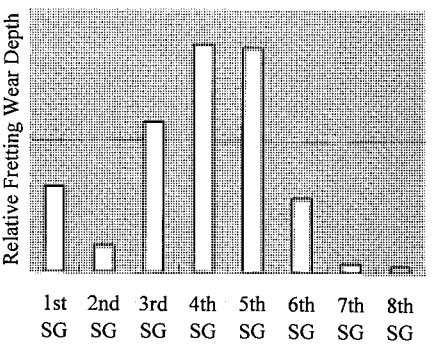


Fig.2 Fretting wear depth profile versus spacer grid observed in a nuclear with the grid-to-rod fretting-induced failure.

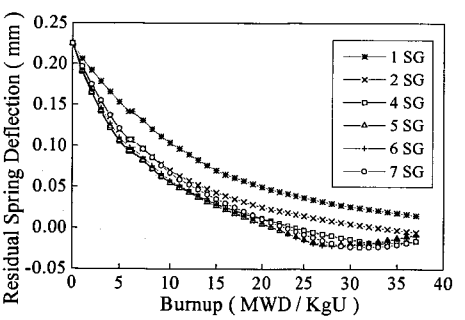


Fig.3 Burnup-dependent residual spring deflection at various grid positions for a fuel type with the fretting wear induced damage, predicted by the GRIDFORCE program.

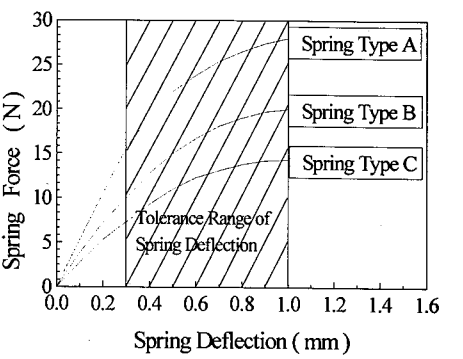


Fig.4 Spring characteristic curves for three spring types used in this work.

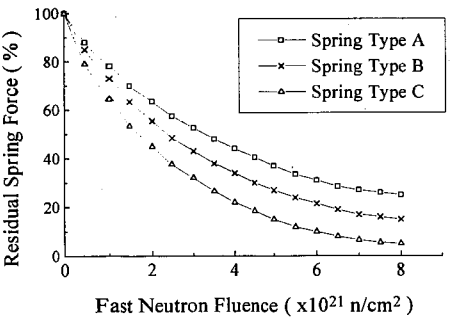


Fig.5 Spring force relaxation rates for three spring types used in this work, derived under a constant total spring deflection condition.

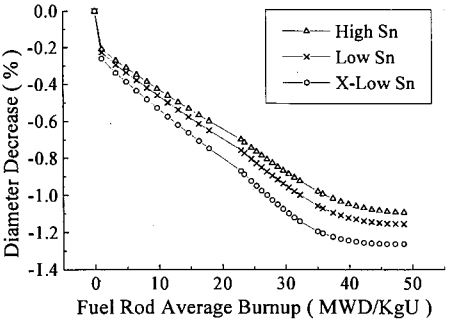


Fig.6 Cladding creepdown rates for three cladding tubes used in this work.

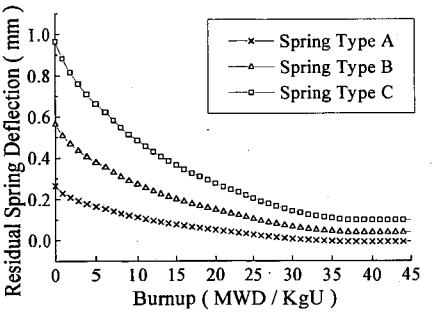


Fig.7 Effect of initial spring deflection on residual spring deflection.

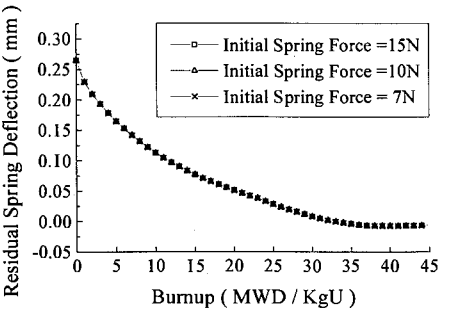


Fig.8 Effect of initial spring force on residual spring deflection.

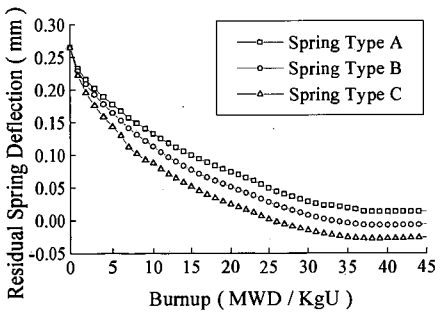


Fig.9 Effect of spring force relaxation rate on residual spring deflection.

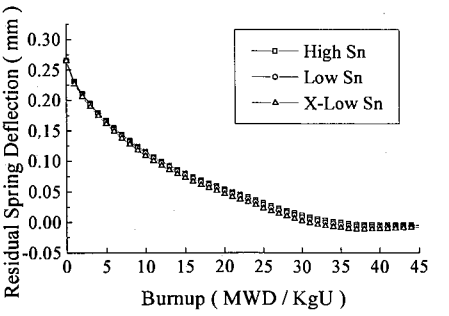


Fig.10 Effect of cladding creepdown rate on residual spring deflection.